ASPECTS OF THE UNITARIZED SOFT MULTIPOMERON APPROACH IN DIS AND DIFFRACTION.

M.B. Gay Ducati[(a)], E.G. Ferreiro[(b)], M.V.T. Machado[(a)], C.A. Salgado[(c)]

[(a)] Instituto de Física, Universidade Federal do Rio Grande do Sul,
Caixa Postal 15051, CEP 91501-970, Porto Alegre, RS, Brazil,
[(b)] Depto. de Física de Partículas, Universidade de Santiago de Compostela
E-15706 Santiago de Compostela, Spain,
[(c)] CERN CH-1211 Geneva 23, Switzerland.

ABSTRACT

We study in detail the main features of the unitarized Regge model (CFKS), recently proposed to describe the small-Q^2 domain. It takes into account a two-component description, which handles with multiple soft Pomeron exchanges contribution, interacting with the large dipole size configurations, and a unitarized dipole cross section, describing the interaction with the small size dipoles. Its extrapolation to higher virtualities is performed, analysing the ratio between soft and hard pieces and discussing the resulting dipole cross section in comparison to that from the saturation model. Diffraction dissociation is also considered, showing the scaling violations in diffractive DIS and estimating the corresponding logarithmic slope.

CERN-TH/2001-265
October 2001.

1 Introduction

The study of a new regime of QCD, that of high density of partons, has drawn much attention in the least years. The key discovery was the observation at HERA of the fast growth of parton densities (mainly gluons) as the energy increases in experiments of deep inelastic scattering. Taking $\sigma^{tot} \sim s^{\alpha(0)-1}$ ($F_2 \sim x^{-\alpha(0)+1}$), values of $\Delta \equiv \alpha(0) - 1$ in the range 0.1 – 0.5 have been reported, depending on the virtuality Q^2 of the photon. However, this steep growth should be tamed, leading to the expected limit given by the Froissart bound ($\sigma \lesssim (\log s)^2$ as $s \to \infty$)[1]. This boundary has been derived from very general properties of the S-matrix, namely unitarity. A cross section growing as any positive power of s would violate unitarity at asymptotic energies. Thus, theoretically, some kind of saturation of this growing due to unitarity effects should be expected [2]. The dynamics of such very dense partonic systems is very interesting and has been studied by many authors both in DIS [3] and in high energy nuclear interactions [4].

The description of the $\gamma^* p$ collision in the frame where the proton is at rest is very appropriate to include unitarity corrections. In this frame, the virtual photon γ^* emitted by the incoming lepton fluctuates into a $q\bar{q}$ pair. This system then suffers multiple interactions with the proton. Such multiple interactions restore unitarity even in the case where it would be violated in a single collision. In the model developed in [5, 6], all these corrections have been taken into account, and their strength is constrained by diffractive data. Therefore, the ratio $\sigma^{diff}/\sigma^{tot}$ is related to unitarity corrections. This is a common feature to any realization of the Gribov model [7], where the amount of rescatterings is related to diffractive production by means of AGK-cutting rules [8].

In parton language, the increasing number of gluons in a proton as $x \to 0$ makes gluon fusion very probable. This fusion produces gluons of higher longitudinal momentum, stopping the growing of those with the smallest x. In this way unitarity is not violated. Such a procedure was implemented on theoretical grounds from QCD through the multiladder exchange in lines of the GLR formalism [3], giving rise to non-linear effects in the standard linear DGLAP approach. The outstanding quantity emerging from the unitarization procedure is the saturation scale $Q_s^2(A, x, b)$, setting the region where saturation phenomenon starts to be meaningful. The QCD-inspired phenomenological model [9], for instance, introduces a quite clear identification for this scale $Q_s^2(x) \sim 1/R_0^2(x)$. There the saturation radius $R_0(x)$, related with the mean transverse distance between partons, is properly extracted from the small-x data from HERA.

In any of the descriptions, unitarity corrections are given by non-linear terms, and a phenomenon of saturation is expected when these terms become important. Since the gluons are the partons driving of the high energy processes, signals for saturation effects should appear in observables probing the gluonic content of the proton (or the nucleus) [10]. In the nuclear case, the gluon density is $\sim A^{1/3}$ higher than in the proton. This makes unitarity corrections more important for nuclei, producing the well-known shadowing of F_2 [11]. Saturation will thus start at smaller energies in nuclei than in protons. Such a fact is the main reason for the increasing interest in the forthcoming eA experiments, where the nucleus will be studied at energies higher than currently available [11].

The open question is if unitarity corrections have already shown up at present energies and if saturation has been reached. In particular, at HERA, they should appear in the small-x and small-Q^2 data [12]. There are several proposals in this direction [9] [13], mainly for the case of heavy-ion collisions [14], but a definitive answer is still missing. The main difficulty that we are faced with is the saturation scale Q_s, lying in the transition interval of 1–2 GeV, which leads the effects to be hidden in more inclusive observables. In this kinematical region the standard QCD perturbative expansion is expected not to be completely reliable. For instance, higher twist terms to the linear approach should take place in such a domain. Moreover, this region is known to hold the interplay between the soft and hard domains, i.e. the perturbative approaches (including saturation or properly adjusting initial conditions) and the Regge-inspired models are competing, and both frameworks seem to describe the current small-x data.

Bearing in mind that the saturation phenomenon is required in a complete understanding of the high energy reactions, and that a consistent treatment of both inclusive and diffractive processes should be taken into account, in this work we study derivative quantities using the Regge unitarized CFKS model [5, 6]. In this hybrid model, both soft (multiperipheral Pomeron and reggeon exchanges) and hard (dipole picture) contributions are properly unitarized in an eikonal way. This approach describes the transition region and can be used as initial condition for a QCD evolution at high virtualities [15]. Its extrapolation to the higher-Q^2 domain is also performed here, discussing the similarities and/or connections with the phenomenological saturation model [9], stressing that a QCD evolution is required for a correct description of higher Q^2 in the inclusive case. For the diffractive case, such a procedure is not formally required, since the non-perturbative sector is dominant in this case. The diffractive structure function is extrapolated to the available larger-Q^2 range. In particular, the diffractive logarithmic slope, which has been claimed as a possible new observable to disentangle dynamics [16, 17], was calculated and compared with the result from the saturation model.

2 The inclusive case

Briefly reviewing the CFKS approach, it interpolates between low and hard virtualities Q^2, which are related to the dipole separation size, r, at the target rest frame, considering a two-component model [5, 6]. Considering the unifying picture of the color dipoles, the soft piece corresponds to the interaction of the asymmetric $q\bar{q}$ pair configurations, the aligned jet case; the hard piece is dominated by the symmetric pair configurations. Hereafter we use the notation *soft* for the asymmetric photon fluctuation (in [6] it is named L) and *hard* for the small size ones (named S in [6]).

The soft component considers multiple soft Pomeron exchange (and reggeon f) implemented in a quasi-eikonal approach [18]. The corresponding diagrams are the fan ones. The initial input is a phenomenological Pomeron with fixed intercept $\varepsilon_{I\!P} = 1.2$ (further changes are due to absorptive corrections), and an exponential parametrization for the t dependence is considered.

In the impact parameter representation, the b-space, it looks like (in photoproduction $Q^2 = 0$):

$$\chi^{I\!P}(s,b) \simeq C_{I\!P} \frac{f_{I\!P}}{B_{el}(s)} \left(\frac{s}{s_0}\right)^{\varepsilon_{I\!P}} \exp[-b^2/B_{el}(s)]\,, \tag{1}$$

where $B_{el}(s)$ is the elastic slope, which is parametrized as in the hadronic reactions. The $f_{I\!P}$ is an effective Pomeron–proton coupling. In the electroproduction case, the initial input is described in an analogous way:

$$\chi^{I\!P}(s,b,Q^2) \simeq \frac{C_{I\!P}}{R(x,Q^2)} \left(\frac{Q^2}{s_0+Q^2}\right)^{\varepsilon_{I\!P}} x^{-\varepsilon_{I\!P}} \exp[-b^2/R(x,Q^2)]\,, \tag{2}$$

corresponding to the Regge parametrization for the amplitude of the soft Pomeron exchange, similar to the Donnachie–Landshoff one [19]. The function $R(x,Q^2)$ comes from the exponential assumption about the t dependence and further transformation to the impact parameter representation. We notice the authors consider a Pomeron fixed intercept taking a semi-hard value rather than a soft one.

The resummation of the triple-Pomeron branches is encoded in the denominator of the amplitude $\chi^{n\,I\!P}$, i.e. the Born term in the eikonal expansion. Moreover, the corrected amplitude is eikonalized in the total cross section,

$$\chi^{n\,I\!P}(x,Q^2,b) = \frac{\chi^{I\!P}(x,Q^2,b)}{1+a\chi_3(x,Q^2,b)}\,, \tag{3}$$

$$\sigma^{n\,I\!P}(x,Q^2,b) \simeq 1-\exp\left[\chi^{n\,I\!P}(x,Q^2,b)\right]\,. \tag{4}$$

where the constant a depends on the proton-Pomeron and the triple-Pomeron couplings at zero momentum transfer ($t = 0$). Refs. [5, 6] give a more detailed discussion.

The eikonalization procedure modifies the growth of the total cross section from a steep power-like behavior to a milder logarithmic increase. The above parametrization corresponds to the interaction with the large size dipole configurations and therefore dominates in low-Q^2 values. The total soft contribution is obtained by integrating over the impact parameter the cross section at fixed b, $\sigma^{n\,I\!P}(x,Q^2,b)$,

$$\sigma^{soft}(s,Q^2) = 4\int d^2b\ \sigma^{soft}(s,Q^2,b)\,. \tag{5}$$

The hard component is considered in the color dipole picture of DIS [20]. The dipole cross section, modeling the interaction between the $q\bar{q}$ pair and the proton, $\sigma^{dipole}(x,r)$, is taken from the eikonalization of the expression above $\chi^{n\,I\!P}(s,b,Q^2)$ already corrected by triple-Pomeron branching (the fan diagrams contributions). The configurations (dipole size) considered are the small transverse distance between the quark–antiquark pair in the dipole. The corresponding cross section is extracted by considering contributions coming from distances between 0 and $r_0 = 0.2$ fm (1 GeV^{-1}), whereas contributions for $r > r_0$ are described by the soft piece already

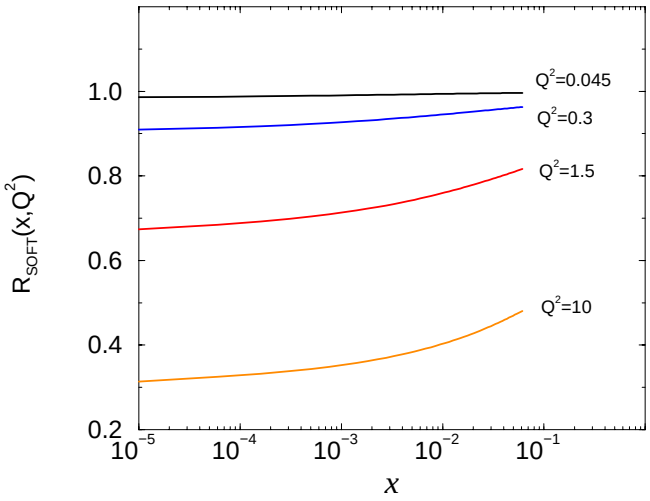

Figure 1: The ratio R_{SOFT} as a function of x at fixed virtualities.

discussed. In such small distances, perturbative QCD is expected to work. The total cross section considering this dipole cross section is expressed as [6]:

$$\sigma_{tot}^{hard}(x,Q^2) = \int_0^{r_0} d^2r \int_0^1 d\alpha \, |\Psi_{\gamma^* q}^{T,L}(\alpha,r)|^2 \, \sigma_{CFKS}^{dipole}(x,r) \,, \tag{6}$$

$$\sigma_{CFKS}^{dipole}(x,r) = 4 \int d^2b \; \sigma^{n\,I\!P}(x,Q^2,b,r) \,, \tag{7}$$

$$\sigma^{n\,I\!P}(x,Q^2,b,r) \simeq 1 - \exp[\, r^2 \chi^{n\,I\!P}(x,Q^2,b) \,] \,, \tag{8}$$

where T and L correspond to transverse and longitudinal polarizations of a virtual photon, $\Psi_{\gamma^* q}^{T,L}(\alpha,r)$ are the corresponding wave functions of the $q\bar{q}$-pair.

A purely QCD phenomenon is introduced in the Born term of the eikonal expansion, presented in the last expression above. The dependence on the radius is introduced *ad hoc* to ensure the correct behavior determined by the color transparency, namely for small r the growth in radius should be proportional to r^2.

The weight of each contribution (soft and hard) for the total cross section [and $F_2(x,Q^2)$] can be obtained, providing a closer analysis of the role played by each piece constituting the model. Such a procedure allows us to explicitate the regions of x and Q^2 where the sectors contribute. In Figs. 1 and 2 we calculate the ratio R_{SOFT}, defining the fraction of the total contribution arising from the soft sector:

$$R_{SOFT}(x,Q^2) = \frac{\sigma_{tot}^{soft}(x,Q^2)}{[\sigma_{tot}^{soft}(x,Q^2) + \sigma_{tot}^{hard}(x,Q^2)]} \,. \tag{9}$$

From Fig. 1 we note that the soft contribution slowly increases as the momentum fraction

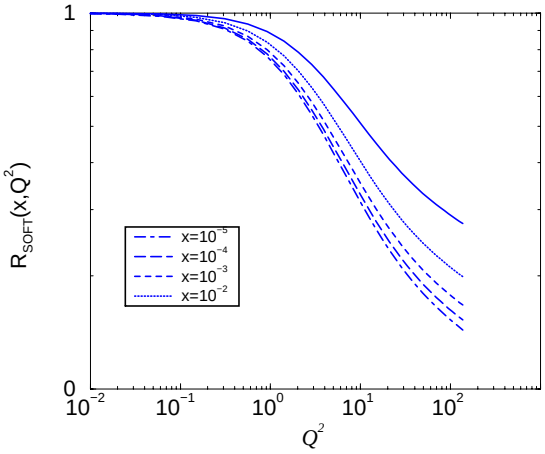

Figure 2: The ratio R_{SOFT} as a function of Q^2 at fixed momentum fraction x.

x goes to higher values, almost independently of the virtuality Q^2. This is due to the fact that higher reggeon trajectories f are included in the soft part, but not in the hard one. Regarding fixed virtualities, the soft piece dominates completely the total cross section at $Q^2 = 0.045$. As Q^2 increases the contribution goes down. For instance, at $Q^2 = 10$ GeV^2 it contributes about half of the cross section. Extrapolating up to higher virtualities, the soft piece saturates at about 5–15% of the total result.

Figure 2 clearly shows that the soft piece is dominant at $Q^2 = 0.01$ and decreases as the virtuality grows. The behavior is monotonic, almost independent of the momentum fraction x. For instance, at $Q^2 = 100$ GeV^2, it contributes with 20% at $x = 10^{-2}$ and 5% at $x = 10^{-5}$. Such a reduction on the soft content is related to the coupling of the photon to the asymmetric dipoles $g^2_{soft}(Q^2) \sim 1/(1 + Q^2/m^2_{soft})$ and to the enhancement in Q^2 provided by the photon wave function (at high $Q^2 \gg Q^2_s(x)$ the symmetric dipole configuration provides the scaling with logarithmic violation).

An interesting issue is the relation between the dipole cross section coming from the CFKS model and the phenomenological one of G.-Biernat-Wüsthoff [9]. The GBW cross section is parametrized as:

$$\sigma^{GBW}(x,r) = \sigma_0 \left[1 - \exp(-r^2/4R_0^2(x))\right] , \quad (10)$$

$$R_0^2(x) = \left(\frac{x}{x_0}\right)^{\lambda} \text{GeV}^{-2} , \quad (11)$$

where $\sigma_0 = 23.03$ mb properly normalizes the dipole cross section. The remaining parameters are $\lambda = 0.288$ and $x_0 = 3.04 \times 10^{-4}$, all of them determined from the small-x HERA data. The $R_0(x)$ is the main theoretical contribution, defining the saturation scale, which is related with the taming of the gluon distribution at small x (unitarity effects) [3]. The above expression has been used to describe both inclusive and diffractive structure functions, in good agreement with the experimental results. The comparison between this approach and the CFKS dipole cross

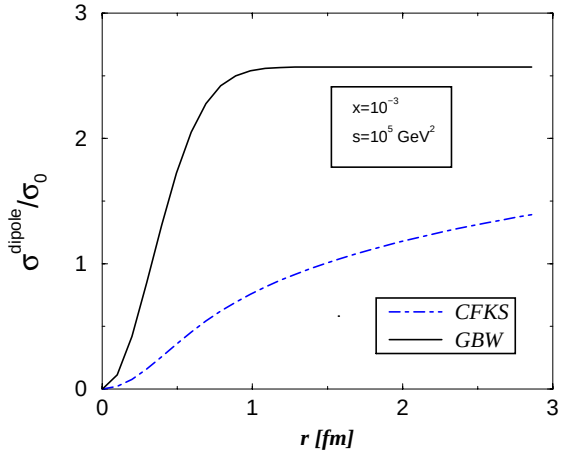

Figure 3: The comparison between the saturation dipole cross section from G.-Biernat-Wusthoff (GBW) and CFKS as a function of the transverse dipole separation r at fixed x (s).

section is shown in Fig. 3. We have plotted the adimensional result, since the normalization for the CFKS dipole cross section, σ_0, is not determined from data. Indeed, for a comparison with experiment using only the hard piece from CFKS, the adjustable parameters would have to be refitted. We consider here that this can be absorbed by a suitable normalization, and carry the r interval beyond the range set by the model ($r < r_0$). The main feature of the GBW parametrization is that it ensures that the dipole cross section grows linearly with r^2 at small transverse separation, whereas it saturates at large size configurations. The picture emerging from the CFKS is slightly different, presenting a mild (logarithmic) increase with r, away from huge separation sizes that shift the saturation scale up to very high virtualities. Although the continuous and smooth increasing with radius, in the CFKS approach the cross section underestimates the GBW one for all r.

A comment on the normalization is in order. The GBW formula would correspond to the hard part of CFKS without triple-pomeron ($a = 0$), and taking a step function for the profile instead of a gaussian. This makes unitarity corrections stronger. In any case, modifying in this way CFKS one obtains $\sigma_0 = \pi R(x, Q^2) \sim 20$ mb, in agreement with GBW value. This value, however, depends logarithmically on x and Q^2, because of the increase of the proton radius, which is taken into account in (2).

3 The diffractive case

The diffractive sector in the CFKS approach is constructed by a three-component model [5, 6], using the AGK cutting rules to relate the elastic multiple scattering amplitude to the inelastic diffractive contribution [8]. The first term comes directly from the soft piece, the second one from the triple-Pomeron (and the reggeon f) interaction and the last one from the hard (dipole)

piece. We notice that these contributions define only the energy, s (and momentum fraction x), and the virtuality dependences. The spectrum on β is introduced by hand, based on earlier soft and hard (pQCD) calculations. The first component is written as:

$$F_{2\,(soft)}^{D}(x,Q^2,\beta) \sim F_{soft}^{D\,(\mathrm{Born})}\, K_L(s,Q^2)\, \beta^{-\varepsilon_{I\!P}}\, (1-\beta)^{n_p(Q^2)}\,, \tag{12}$$

where $F^D\,(\mathrm{Born})_{soft} \sim \chi^{n\,i}(s,Q^2)\chi^{n\,k}(s,Q^2)$ is the lowest-order (Born) approximation for that function, with $i,k = I\!P, f$. The suppression factor due to higher order multipomeron exchanges is $K_L(s,Q^2) = \sigma_{soft}^{(0)}/\sigma_{soft}^{(0)\,\mathrm{Born}}$, with $\sigma_{soft}^{(0)} = 4g_L^2(Q^2)\int d^2b\,[\sigma_{soft}(s,Q^2,b)]^2$. Further details can be found in [6]. The β dependence is taken from the typical CKMT Pomeron structure function, which is connected with the deuteron structure function by the identification $x \to \beta$ [21].

The hard contribution is expressed as:

$$F_{2\,(hard)}^{D}(x,Q^2,\beta) \sim \sigma_{hard}^{(0)\,T}\,\beta^3(1-2\beta)^2 + \sigma_{hard}^{(0)\,L}\,\beta^2(1-\beta)\,, \tag{13}$$

where the β dependence comes from a pQCD guess for the Pomeron structure function [22]. Also, $\sigma_{hard}^{(0)\,T,L} = \int d^2b\,[\sigma_{hard}^{T,L}(s,Q^2,b)]^2$. However, the β spectrum is slightly different from the most recent pQCD calculations, where the transverse contribution behaves like $\sim \beta(1-\beta)$ and the longitudinal one as $\sim \beta^3(1-2\beta)^2$ [23].

Regarding the β dependence, the region for medium values ($\beta \sim 0.4$) is dominated by the soft term, which in pQCD is associated to the transverse photon contribution [23]. The small β region is dominated by the triple-Pomeron piece, in agreement with the pQCD expectations, which is obtained by considering the higher twist $q\bar{q}$+gluon configuration. Moreover, the hard contribution is leading in the large-β region, associated in this case with a suppression of the transverse contribution and an enhancement of the longitudinal piece in comparison with the expected pQCD behavior [23].

The CFKS approach describes with good agreement the diffractive DIS data in the broad range $0 < Q^2 < 18$ GeV^2. In order to study the model in comparison with the pQCD approaches, here we extrapolate the prediction for the diffractive structure function of the CFKS approach for higher values of the virtuality. We use the preliminary ZEUS analyses, considering the Q^2 dependence at fixed mass M_X and centre-of-mass energy W [24]. These data provide information at both small and large virtualities bins. An interesting comparison is between the CFKS model and the saturation model [9] prediction for the diffractive structure function. Both models are depicted in the plots of Fig. 4.

The agreement of CFKS approach with data is noticeable even at higher virtualities, where the model is expected not to be reliable. However the interpretations at low Q^2 are quite different. In the saturation model, the reliability of the pQCD calculation is extended to smaller virtualities through the saturation scale $R_0(x)$ and where the dependence is mostly due to the longitudinal photon configuration and by the higher twist $q\bar{q}$+gluon. Instead, in the CFKS model the main contribution in the region of interest comes from the soft triple-Pomeron contribution.

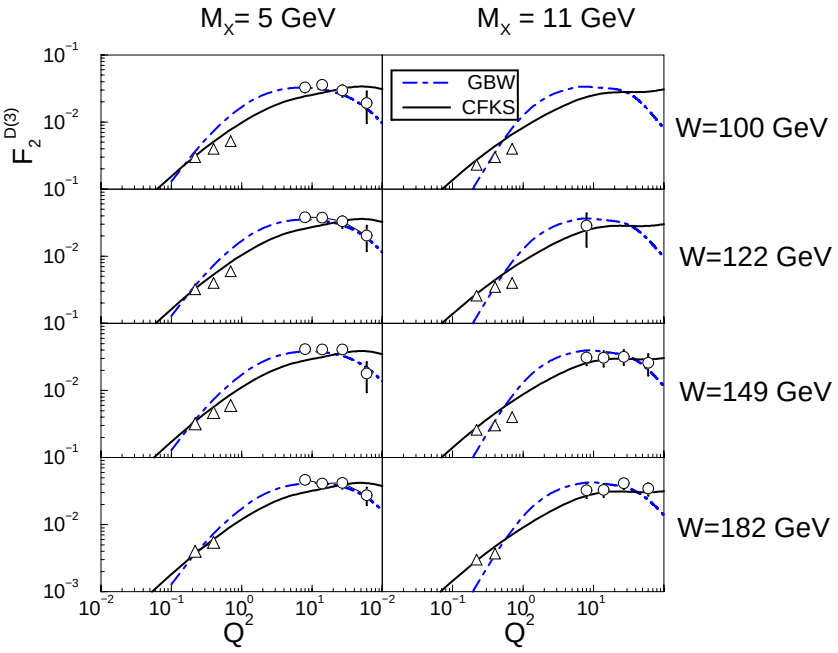

Figure 4: The diffractive structure function as a function of Q^2 at fixed M_X and W. The preliminary data are from ZEUS Collaboration (triangles). The published data are the circles. The CFKS and GBW results are shown in the same plot.

As a final study, we perform the calculation of the Q^2 logarithmic slope of the diffractive structure function $F_2^{D(3)}$. The motivation is that this observable is a potential quantity to distinguish soft and hard dynamics in diffractive DIS [16, 17]. We have calculated the slope as a function of the Pomeron momentum fraction $x_{I\!P}$ and perform a comparison between the CFKS approach and the G.-Biernat-Wusthoff (GBW) one.

Here, some comments are in order. The main feature of the GBW approach is the presence of a transition between positive and negative slope signals, instead of a predominantly positive slope, as in the pQCD non-saturated case [17]. The transition is not present in the pQCD model without saturation because of the assumptions made in the parametrization of the HERA data in the region of large Q^2 (large β). We notice that this situation can be changed by further reanalysis, considering the updated runs at the H1 experiment, which has enlarged the kinematical range and news measurements [25]. It is important to emphasize that a transition is verified in the preliminary ZEUS analyses of diffractive DIS [24] , where the saturation model [9] is considered to describe the Q^2 dependence of the diffractive structure function, using as kinematical variables M_X and W rather than β and $x_{I\!P}$. Such a procedure is performed because of the similarity of the behaviors of $d\sigma/dM_X$ and $\sigma_{tot}(\gamma^* p)$ in the same kinematic range. In that analysis, the growth of $x_{I\!P} F_2^D$ versus Q^2 is stopped at $Q^2 \sim 10$ GeV^2 and decreases smoothly for larger virtuality values. The transition region corresponds to $\beta \sim 0.2$ for $M_X = 5$ GeV and $\beta \sim 0.07$ for $M_X = 11$ GeV.

The saturation model produces a transition between positive and negative slope values at low $\beta = 0.04$, while it presents a positive slope for medium and large β. Instead, the CFKS

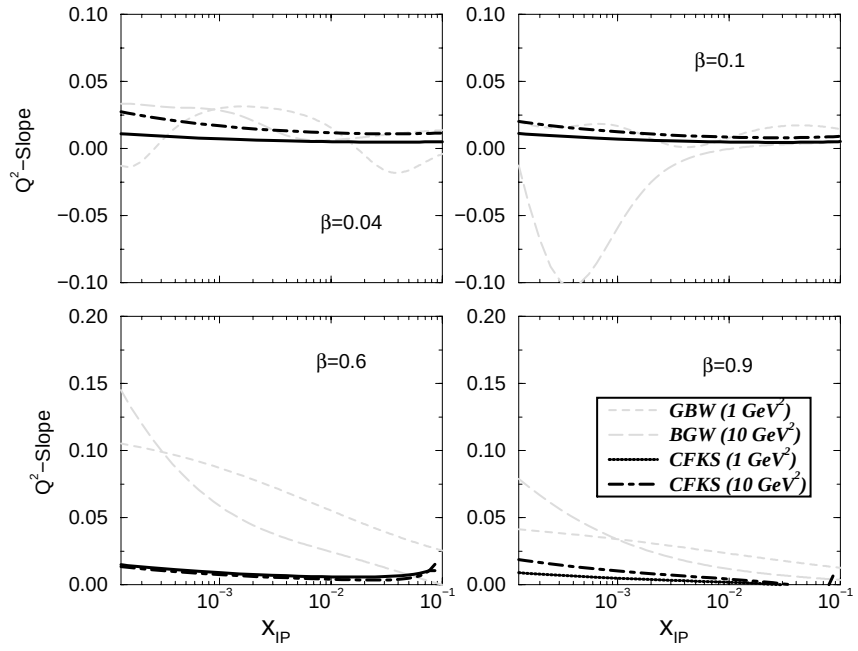

Figure 5: The Q^2 logarithmic slope of the diffractive structure function as a function of $x_{I\!P}$ at fixed β and analysed on the virtualities Q^2. The CFKS and GBW results are shown in the same plot.

approach shows a positive slope for the whole Q^2 and $x_{I\!P}$ ranges, flattening at large β, much in the same way as the non-saturated pQCD calculations.

4 Conclusions

A deeper understanding of the saturation phenomenon is required to perform reliable estimates for the current and forthcoming high energy reactions. The saturation scale, which sets the onset of the unitarity corrections, is found to be lying in the transition regime of low x and Q^2. In this domain, both Regge-inspired phenomenology and improved pQCD calculations (perturbative shadowing, higher twist), considering unitarity effects, are able to describe the high precision data. The most advantageous ones are those describing in an unified way the inclusive processes as well as diffractive ones. In this letter we have considered the two-component multireggeon model of [5, 6] and calculated some derivative quantities.

The ratio of the soft content in the model was calculated, verifying that it dominates at low Q^2, diminishing at higher virtualities. This shows that the unitarity corrections in this model are more important in the soft component than in the hard one. Moreover, these corrections are higher twist at large Q^2 in the second case.

It remains the issue if the model is able to describe a larger range in Q^2 without to consider a pQCD evolution. A good hint to answer this question is to analyse the hard piece (symmetric

dipole configurations), in particular the corresponding dipole cross section. We have found that the saturation in r of this quantity lies at values of the radius bigger than the phenomenological GBW model. A similar consideration is far from clear for the diffractive case, where non-perturbative (soft) content plays a more important role.

We have extrapolated the estimates for the diffractive structure function at higher virtualities. It was verified that a broad description is obtained, and that it is in reasonable agreement with the saturation pQCD model. An additional quantity has been proposed in order to describe dynamics at diffractive dissociation [16, 17], namely the diffractive slope. It is calculated using the CFKS model, and its main feature is a similar behavior to the one predicted by pQCD calculations [23].

Acknowledgements

M.B.G.D and M.V.T.M are supported by CNPq and by PRONEX (Programa de Apoio a Núcleos de Excelência), Brazil. C.A.S. is supported by a Marie Curie Fellowship of the European Community programme TMR (Training and Mobility of Researchers), under the contract number HPMF-CT-2000-01025.

References

[1] M. Froissart, *Phys. Rev.* **123**, 1053 (1961);
A. Martin, *Phys. Rev.* **129**, 1462 (1963).

[2] A.H. Mueller, *Nucl. Phys.* **B335**, 115 (1990).

[3] L.V. Gribov, E. M. Levin, M.G. Ryskin, *Phys. Rep.* **100**, 1 (1983);
A. L. Ayala, M.B. Gay Ducati and E. Levin, *Nucl. Phys.* **B493**, 305 (1997); **B511**, 355 (1998);
Y. U. Kovchegov, *Phys Rev.* **D60**, 034008 (1999).
I. Balitsky, *Nucl. Phys.* **B463**, 99 (1996).

[4] L. Mc Lerran and R. Venugopalan, *Phys. Rev.* **D49**, 2233, 3352 (1994); **50**, 2225 (1994); **53**, 458 (1996);
E. Iancu, A. Leonidov and L. Mc Lerran, *Phys. Lett.* **B510**, 133 (2001); Nucl. Phys. A **692**, 583 (2001);
E. Ferreiro, E. Iancu, A. Leonidov and L. McLerran, [hep-ph/0109115].
J. Jalilian-Marian *et al. Phys. Rev.* **D59**, 034007 (1999);
N. Armesto and M. A. Braun, *Eur. Phys. J.* **C20**, 517 (2001); [hep-ph/0107114];
A. Kovner and U. A. Wiedemann, [hep-ph/0106240].

[5] A. Capella, E.G. Ferreiro, A.B. Kaidalov and C.A. Salgado, *Nucl. Phys.* **B593**, 336 (2001).

[6] A. Capella, E.G. Ferreiro, A.B. Kaidalov and C.A. Salgado, *Phys. Rev.* **D63**, 054010 (2001).

[7] V. N. Gribov, *ZhETF* **57**, 654 (1967).

[8] V.A. Abramovsky, V.N. Gribov and O.V. Kancheli, *Sov. J. Nucl. Phys.* **18**, 308 (1974).

[9] K. Golec-Biernat and M. Wüsthoff, *Phys. Rev.* **D59**, 014017 (1999); **D60**, 114023 (1999).

[10] A.L. Ayala, M.B. Gay Ducati, V.P. Gonçalves, *Phys. Rev.* **D59**, 054010 (1999).

[11] M.B. Gay Ducati, V.P. Gonçalves, *Phys. Lett.* **B466**, 375 (1999).

[12] A.L. Ayala, M.B. Gay Ducati, E.M. Levin, *Phys. Lett.* **B388**, 188 (1996).

[13] M. McDermott, L. Frankfurt, V. Guzey and M. Strikman, *Eur. Phys. J.* **C16**, 641 (2000);
N. Armesto and C. A. Salgado, [hep-ph/0011352] (*Phys. Lett.* **B** to appear);
E. Gotsman *et al.*, [hep-ph/0010198].

[14] K. J. Eskola, K. Kajantie, P. V. Ruuskanen and K. Tuominen, *Nucl. Phys.* **B570**, 379 (2000);
K. J. Eskola, K. Kajantie and K. Tuominen, *Phys. Lett.* **B497**, 39 (2001);
D. Kharzeev and M. Nardi, *Phys. Lett.* **B507**, 121 (2001);
D. Kharzeev and E. Levin, [nucl-th/0108006];
A. Capella and D. Sousa, *Phys. Lett.* **B511**, 185 (2001);
A. Krasnitz and R. Venugopalan, *Phys. Rev. Lett.* **86**, 1717 (2001); **84**, 4309 (2000);
A. Accardi, [hep-ph/0107301].

[15] A. Capella, A.B. Kaidalov and C.A. Salgado, in preparation.

[16] M.B. Gay Ducati, V.P.B. Gonçalves and M.V.T. Machado, *Phys. Lett.* **B506**, 52 (2001).

[17] M.B. Gay Ducati, V.P.B. Gonçalves, M.V.T. Machado, hep-ph/0103245 (*Nucl. Phys.* **A** in press).

[18] K.A. Ter-Martirosyan. *Nucl. Phys.* **B36**, 566 (1972).

[19] A. Donnachie and P. V. Landshoff, Phys. Lett. B **296**, 227 (1992); B **437**, 408 (1998).

[20] N. Nikolaev and B.G. Zakharov, *Z. Phys.* **C49**, 607 (1990).
N. Nikolaev, E. Predazzi and B.G. Zakharov, *Phys.Lett.* **B326**, 161 (1994).
J.R. Forshaw and D.A. Ross, *Quantum Chromodynamics and the Pomeron*, Cambridge University Press, 1997.

[21] A. Capella *et al.*, *Phys. Lett.* **B343**, 403 (1995).
A. Capella *et al.*, *Phys. Rev.* **D53**, 2309 (1996).

[22] J. Bartels, L.L Frankfurt and M. Strikman, *Phys. Rep.* **160**, 235 (1988).

[23] J. Bartels and M. Wüsthoff, *J. Phys. G: Nucl. Part. Phys.* **22**, 929 (1996);
J. Bartels *et al.*, *Eur. Phys. J.* **C7**, 443 (1999).

[24] ZEUS Collaboration, *Eur. Phys. J.* **C6**, 67 (1999).
ZEUS Collaboration, *Measurement of the diffractive cross section at* $Q^2 < 1\,GeV^2$ *at HERA*, in Proc. ICHEP2000, Osaka, Japan (2000) [plenary session 12, paper 435].

[25] H1 Collaboration, *Measurement of the Diffractive Structure Function* $F_2^{D(3)}(x_{I\!P}, \beta, Q^2)$ *at HERA*, in Proc. Conference EPS2001 Budapest, July 12 (2001); and in Proc. Conference Lepton-Photon2001, July 23 (2001).